Musculoskeletal Research Center

Summer Research Program

2013

University of Pittsburgh

Department of Bioengineering

MSRC

Table of Contents

2013 Abstract Book Committee

Connie Chen, Hunter Eason

The efforts and findings displayed in this abstract book represent the labors of the 2013 summer interns at the Musculoskeletal Research Center. Through this experience, we have come to appreciate the dedication demonstrated year-round by the members of the MSRC. It is with our deepest sincerity and gratitude that we thank them for their generosity with their time and the knowledge that they have passed on. In addition to gaining knowledge applicable to our fields of study, we have also received valuable guidance regarding our writing, analysis of scientific literature, and presentation skills.

On behalf of all of the interns, I would like to thank the MSRC faculty for the opportunity to benefit from the patience and countless resources that have formed this incredibly instructional learning environment. Furthermore, we would like to especially thank Dr. Woo, Dr. Abramowitch, and our graduate student mentors for opening up their work to us. The time that we have committed here has provided a challenging, rewarding experience that has given us new knowledge and skills which we will surely take with us to the next stages of our lives.

- Connie Chen, Editor

2013 Summer Symposium Chairwoman

Aimee Pickering

This year the Summer Student Symposium was held on July 19th, 2013 at the Musculoskeletal Research Center. Each student received the opportunity to present the project that they had worked on for the past 7-9 weeks. At the end of each presentation, fellow students and MSRC faculty and staff posed questions for the student to test the depth of their knowledge. For many of us it was the first time that we had seen the projects that our fellow interns had been working on. With each of us coming in with little to no knowledge of the specific field that we were asked to do research in, the presentations showed how much every one of us had learned through this opportunity. We have gained skills from this experience, not just in the lab room, but on the presentation floor as well. I know these lessons will follow each of us from this day forward.

On behalf of the symposium committee, I would like to thank everyone who assisted for their help in making the symposium a success. I would especially like to thank Dr. Woo for granting us this opportunity to work in the MSRC.

-Aimee Pickering, Symposium Committee Chairwoman

The MSRC Faculty

Savio L-Y. Woo, Ph.D., D.Sc., D.Eng.
Professor and Director of the MSRC

Patrick McMahon, MD
Adjunct Associate Professor

Steven D. Abramowitch, Ph.D.
Assistant Professor

Connie Chen

University of Pittsburgh

Major: Bioengineering

COC11@pitt.edu

Lab Mentor: Kwang Kim, B.S.

Faculty Advisor: Savio L-Y. Woo, Ph.D., D. Sc., D. Eng.

I was born on November 1, 1991 in Baltimore, MD. My father is an anesthesiologist, and my mother is a stay-at-home mom. I have a younger sister and a younger brother. I graduated from Dallastown High School, where I was a member of the Volunteer Club, Student Director of three school musicals, a Spanish teacher at an elementary after-school program, and a "Big Sister" for Big Brothers/Big Sisters of Central PA for three years. I hope to serve as a physician one day. My aptitude for analysis and problem solving, as well as my mathematical inclination, led to my decision to major in Bioengineering.

I am embarking on my senior year and plan to graduate in 2014. While at the University of Pittsburgh, I have been active as a volunteer in the family ministry of my church and a Patient Navigator at UPMC. I am also going on my third year as an undergraduate chemistry TA and I am a sister of Sigma Delta Tau, for which I have been a Standards Board Chairwoman and currently Treasurer. I am also Business Manager of Global Brigades, an international holistic and sustainable development organization. This past May, we went to Honduras, where we served 900 patients in a medical clinic and helped implement a system which will bring clean water to communities.

From my first day at the MSRC, I have enjoyed the challenge to gain knowledge and be proactive rather than simply follow instructions. I have worked under Kwang Kim, who has been my greatest source of guidance in my time here. I would also like to thank Bill Barone and Dr. Abramowitch, who have been extremely helpful in teaching me about experimental setup and viscosity theory/analysis. Lastly, I would like to thank Dr. Woo for teaching us difficult but important lessons about the value of thorough, independent thinking and taking initiative in research.

MECHANICAL AND VISCOELASTIC PROPERTIES OF THE MEDIAL PATELLOFEMORAL LIGAMENT

Connie Chen, Kwang Kim, B.S., Savio L-Y. Woo, Ph.D., D.Sc., D.Eng.

Musculoskeletal Research Center, Department of Bioengineering, University of Pittsburgh

INTRODUCTION

Acute patellar dislocation is a disorder which frequently affects athletic persons ages 14-20 [1], more often in females. These represent up to 40% of knee injuries [2]. The primary mechanism of injury is a noncontact force to a flexed knee in valgus, when the foot is planted and internal rotation is applied [1]. Patellar dislocation results in recurrent anterior knee pain due to misalignment. However, up to 50% of patients report subsequent pathological conditions, such as residual instability, injury to the articular surface, and posttraumatic arthritis. Sequelae occur especially in young, active people [3].

Surgical treatment is recommended for recurring dislocations, which occurs in 44% of patients [4].The most popular surgical intervention is reconstruction of the medial patellofemoral ligament (MPFL) [5]. The MPFL is the primary medial restraining tissue for the patella. When the patella is laterally displaced, the MPFL is the first ligament to be engaged, contributing up to 50% of the medial restraining force [3]. Over one hundred methods of surgical patellofemoral stabilization have been recorded [6]. However, a major consideration factor for reconstruction, the behavior of the MPFL substance, has been overlooked except for one study which found the ultimate load of the human MPFL [7]. However, no studies have been performed on the mechanical properties of the MPFL, such as tangent modulus, tensile strength, ultimate strain, and strain energy density.

In addition to mechanical properties, ligaments also exhibit viscoelastic properties. QLV theory, as developed by Fung in 1972, is a viscoelastic model for soft tissues that has been validated for ligament substance. QLV theory fits stress-relaxation behavior to a mathematical model. The characteristic constants of QLV theory are as follows [8]:

- B: rate of change of stress/strain curve slope
- $A \times B$: initial slope of stress/strain curve
- C: magnitude of viscous effects present
- τ_1: time constant governing initial relaxation
- τ_2: time constant governing late relaxation

A method developed by for slow-strain rate determination of QLV constants incorporates these constants into the stress-relaxation equation

$$\sigma(t) = \frac{AB\gamma}{1 + C\ln\left(\frac{\tau_2}{\tau_1}\right)} \int_0^t \left\{1 + C\left(E_1\left[\frac{t-\tau}{\tau_2}\right] - E_1\left[\frac{t-\tau}{\tau_1}\right]\right)\right\} e^{B\gamma\tau} d\tau$$

which describes stress-relaxation with time during a static stress-relaxation test. E_1 is the exponential integral [9].

Mechanical and viscoelastic properties give insight into the ligament behavior. In order to choose the best graft for MPFL reconstruction, the graft material with properties closest to that of the MPFL should be considered. The first objective of this study was to determine the mechanical properties of the MPFL. The second objective was to determine the viscoelastic properties of the MPFL using QLV theory and obtain its QLV constants.

MATERIALS AND METHODS

10 fresh frozen pig knees were used for this study. Prior to dissection, they were thawed at room temperature. All soft tissues surrounding the Patella-MPFL-Femur complex were removed. The MPFL segments were excised using a ligament punch with an aspect ratio of 5.5.

First, a water tank is affixed to the materials testing machine (model 5565; Instron, Canton, MA) and filled with a saline bath. A water heater maintains 32°C. The ligament is secured in clamps. Using a laser micrometer, three cross-sectional area measurements are made and averaged. Two strain tracking markers are applied to the ligament with 3 mm separation centered about the ligament midline. The ligament segment is immersed in the saline bath, aligned with the loading axis of the Instron (see Figure 1), and allowed to equilibrate for 30 minutes.

All loading in the following tensile testing protocol occur at a rate of 2 mm/min. The specimen was preloaded to 0.25 N and then subjected to 20 cycles of cyclic preconditioning between 0-0.4 mm of extension. 1 hour recovery was allowed prior to a single static stress-relaxation test, at an elongation of 0.6 mm for 30 minutes. Another hour recovery time was given before 30 cyclic loading cycles between 0.4-0.6 mm. Finally, a load to failure test was applied (see Figure 2)

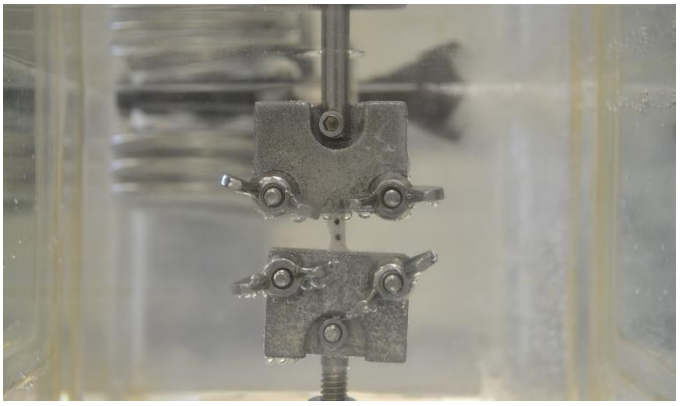

Figure 1. The MPFL as affixed in the materials testing machine. It has two strain tracking markers and is submerged in a saline bath that is heated to 32ºC. The fibers of the MPFL are aligned with the loading axis of the Instron.

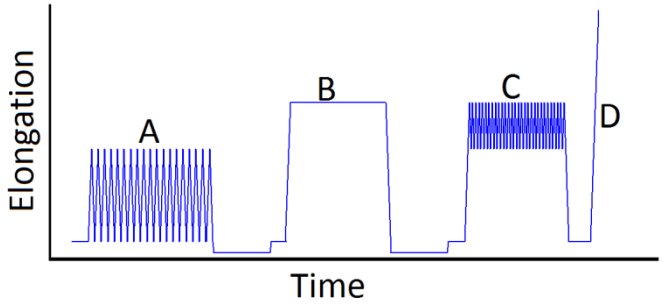

Figure 2. Tensile testing protocol (not to scale), elongation vs. time. Section A displays the cyclic preconditioning between 0-0.4 mm, 20 cycles. Section B displays the static stress-relaxation test a 0.6 mm. Section C demonstrates the cyclic loading test between 0-0.6 mm, 30 cycles. Section D shows the load to failure test.

Throughout the tensile testing protocol [10], the Instron provides load and overall displacement data. During the load to failure test, a camera tracked the displacement of the strain markers. Strain was determined via Mathematica. Mechanical properties as determined from the load-to-failure stress/strain curve were determined in Matlab. QLV properties were also obtained from a code in Mathematica.

RESULTS

The following preliminary data are from a single specimen.

At a strain rate of 2 mm/min, this specimen showed a strain rate of 0.50%/s. The results of the stress/relaxation test are shown in Figure 3. The specimen observed 25.5% stress/relaxation over time. The QLV constants found from this curve are as follows: A was 3.22 MPa, B was 22.1, C was 0.105, τ_1 was 0.44 s, and τ_2 was 1230 s. From these values, peak and valley stresses during cyclic loading could be estimated. They are compared with the actual values in Figure 4.

Figure 3. Results of Stress-Relaxation Test

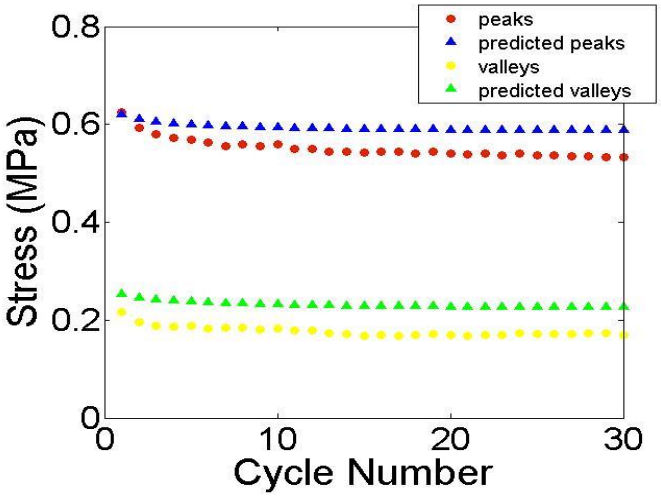

Figure 4. Predicted vs. actual peaks and valleys.

The stress-strain curve produced from the specimen is shown below in Figure 5. Mechanical properties are as follows: tangent modulus of 265 MPa, strain energy density of 1.36 MPa, tensile strength of 23.6 MPa, and ultimate strain of 0.132. The tangent modulus was determined between 4% and 8% strain. The observed cross sectional area was 1.42 mm^2.

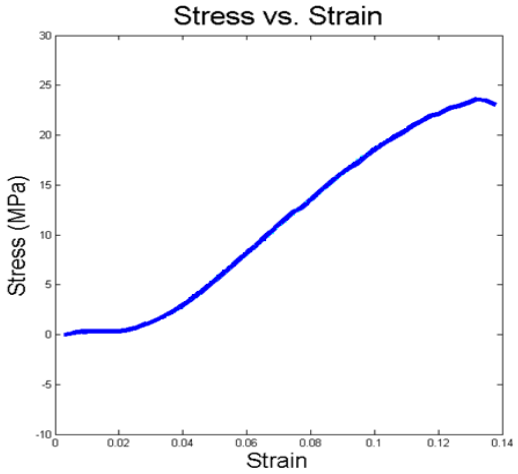

Figure 5. Stress vs. Strain curve for load to failure of specimen.

DISCUSSION

As stated above, commonly used tendons for MPFL construction are semitendinosus and gracilis tendons. Table 1 [10] compares the properties of the porcine MPFL to the proximal and distal segments of human semitendinosus and gracilis tendons.

The MPFL has a lower tangent modulus, strain energy density, and tensile strength than semitendinosus and gracilis tendons but a similar ultimate strain. If the ligament tested was a reliable representative of all porcine MPFL substance, then it is implied that porcine MPFL responds to the same strain levels with significantly lesser stress, and therefore less energy absorbed at failure, than these common MPFL grafts. If human MPFL, as that of a porcine's, has a lower tensile strength than the common grafts, then the use of semitendinosus and gracilis grafts may be beneficial because the graft is less likely to fail.

The determined QLV constants, as compared to the properties of Goat MCL, as found in [10]. This comparison is made solely to get an idea of where the results of this study fall in comparison to previously conducted studies on other animal knee ligaments. The QLV properties found for the pig MPFL specimen fall between that of a healing and a sham-operated goat MCL. This indicates that the QLV constants found from the protocol used are of reasonable values.

Table 1. Comparison of mechanical properties: Porcine MPFL vs. human semitendinosus and gracilis tendons. ST stands for semitendinosus, G stands for gracilis, "prox" indicates proximal, and "dist" indicates distal.

Property	Tangent Modulus (MPa)	Strain Energy Density (MPa)	Tensile Strength (MPa)	Ultimate Strain
Porcine	265	1.36	23.6	0.132
ST(Prox)	446.5	2.6	37.2	0.134
ST(Dist)	484.5	3.4	48.5	0.141
Grac(Prox)	467.5	2.2	34.7	0.113
Grac(Dist)	625.5	4.3	63	0.136

The greatest drawback of this study was the lack of specimens which successfully provided stress-strain data. These results are therefore not reliable. In almost all tests conducted, the specimen failed above the strain markers, near the clamp head. This is likely because the ligament segment used was extremely small and fragile, due to the nature of the punch.

The next course of action is to use a new ligament punch which will allow excision of a larger segment of ligament and still maintain an appropriate aspect ratio for tensile testing. A larger ligament segment will require new loading rates and elongation limits to maintain similar tensile testing strain rates. The ultimate goal of this study is to move on to human MPFLs, after the methodology is fully refined for porcine MPFLs.

ACKNOWLEDGMENTS

I would like to thank the University of Pittsburgh's Honors College Brackenridge Fellowship for its financial support this summer.

REFERENCES

[1] Willis, R.B., and G. Firth, 2012. "Traumatic Patellar Dislocation: Loose Bodies and the MPFL." *J Pediatr Orthop*. 32 pp. 47-51.

[2] Zaffagnini, S., Giordano, G., Bruni, D., Muccioli, G.M.M., and M. Marcacci., 2010. "Pathophysiology of Lateral Patellar Dislocation." *Patellofemoral Pain, Instability, and Arthritis* eds., S. Zaffagnini, D. Dejour, E.A. Arendt, Springer-Verlag, Berlin, pp. 17-27.

[3] Hautamaa, P.V., Fithian, D.C., Kaufman, K.R., Daniel, D.M., and A.M. Pohlmeyer, 1998. "Medial Soft Tissue Restraints in Lateral Patellar Instability and Repair." *Clinical Orthopaedics and Related Research*. 349, p. 174-182.

[4] Steensen, R.N., Dopirak, R.M., and W.G. McDonald, 2004. "The Anatomy and Isometry of the Medial Patellofemoral Ligament: Implications for Reconstruction." *Am J Sports Med*. 32(6), pp. 1509-1513.

[5] Schepsis , A.A., and A.J. Rogers, 2012. "Medial Patellofemoral Ligament Reconstruction: Indications and Technique." *Sports Med Arthrosc Rev*. 20(3), pp. 162-170.

[6] Petersen., W., Forkel, P., Achtnich, A, 2012. "Chronic Patellofemoral Instability." *Unfallchirurg*. 115, pp. 397-409.

[7] Mountney, J., Senavongse, W., Amis, A.A., Thomas, N.P., 2005. "Tensile strength of the medial patellofemoral ligament before and after repair or reconstruction." *J Bone Joint Surg Br*. 87(1) pp. 36-40

[8] Fung, Y.C., 1972, "Stress Strain History Relations of Soft Tissues in Simple Elongation." *Biomechanics: Its Foundations and Objectives* eds., Y.C. Fung, N. Perrone, and M. Anliker, PrenticeHall, Englewood Cliffs, NJ, pp. 181-207.

[9] Abramowitch, S.D., and S. L-Y. Woo, 2004. "An improved method to analyze the stress relaxation of ligaments following a finite ramp time based on the quasi-linear viscoelastic theory." *J. Biomech. Eng.* 126(1) pp. 92-97.

[10] Abramowitch, S.D., Kilger R., Liang, R., and S. L-Y. Woo, 2003. "An Evaluation of the Quasi-Linear Viscoelastic Properties of the Healing Medial Collateral Ligament in a Goat Model." *Annals of Biomed. Eng.* 32(3) pp. 329-335.

[11] Abramowitch, S.D., Zhang, X., Curran, M., and R. Kilger, 2010. "A comparison of the quasi-statis mechanical and non-linear viscoelastic properties of the human semintendinosus and gracilis tendons." *Clinical Biomech*. 25(4) pp. 325-331.

Hunter Eason

University of Pittsburgh
Major: Bioengineering
Senior
Hse1@pitt.edu

Lab Mentor: Katie Farraro, B.S., M.S.
Faculty Advisor: Savio L-Y. Woo, Ph.D., D. Sc., D. Eng.

I was born on November 9, 1990 in Orlando, FL. My family has since moved numerous times and I have lived in South Carolina, Virginia, Illinois, Texas and Pennsylvania. I graduated in Lancaster, PA from the Manheim Township High School where I participated in the school newspaper, track and field, football, and the Junior Engineering Team (JETs). I was also the vice-president of the National Honors Society at my high school. While there, I was an active participant in Boy Scouts and earned my Eagle Scout award during my senior year of high school. I decided to attend the University of Pittsburgh during my senior year to study bioengineering.

At the University of Pittsburgh I have been an active member of a number clubs and societies. This upcoming year, my fifth at the University of Pittsburgh, I will be the president of Tau Beta Pi, the engineering honors society, and the social chair of the Biomedical Engineering Society (BMES). During my sophomore and junior year I was a preceptor for the Fessenden Honors Engineering Program in which I mentored in coming freshmen engineering students as they adapted to college. In addition, since sophomore year I have been an undergraduate teaching assistance for the general chemistry labs at the University of Pittsburgh. One of my most rewarding college experiences was when during the spring semester of my junior year I had the opportunity to study abroad in Dublin, Ireland. Finally, I am currently applying to medical school and am looking forward to attending medical school next year.

I have been a member of the Musculoskeletal Research Center (MSRC) for the last three years. During this time I have worked on the magnesium (Mg)-based ring project under my graduate mentor, Katie Farraro. I have enjoyed working at the MSRC because I have had the opportunity to work with outstanding researchers during my time at the research center. Dr. Woo's guidance and ability to share his knowledge and personal philosophy on both research and life has been very helpful and I am extremely glad I have had the opportunity to perform research in his research center. This summer I was awarded the Brackenridge Summer Research Fellowship from the University of Pittsburgh Honors College, which has funded my research for the summer. I am very thankful for the support of all the graduate students, faculty, and other undergraduate interns of the MSRC over the past three years for their support and am excited to take what I have learned into my career.

CYCLIC LOADING OF A MG-BASED RING REPAIRED ANTERIOR CRUCIATE LIGAMENT

Hunter Eason, Katie Farraro, M.S, Savio L-Y. Woo, Ph.D., D. Sc., D. Eng.
Musculoskeletal Research Center, Department of Bioengineering, Swanson School of Engineering, University of Pittsburgh

INTRODUCTION

The anterior cruciate ligament (ACL) is a commonly injured knee ligament. Due to its low healing capacity, ACL tears are often repaired by surgical reconstruction using a soft tissue autograft or allograft with the goal of restoring joint stability and function. However, studies of reconstructions 10 or more years post-surgery show a significant number of complications including donor site morbidity and osteoarthritis [1,2]. Recent advances in functional tissue engineering have increased interest in ACL healing as an alternative to ACL reconstruction. ACL healing is appealing because it could avoid complications associated with ACL reconstruction while maintaining the ACL's complex geometry and proprioception and removing the need for large bone tunnels.

Studies using biological augmentation such as platelet-rich plasma (PRP) and stem cells to heal the injured ACL have yielded promising results [3,4]. In our research center, we successfully healed a fully transected goat ACL at 12 weeks using an extracellular matrix sheet along with its hydrogel [5]. However, as the ACL healing process is slow, mechanical augmentation is also needed to both provide joint stability and load the ACL insertion sites to prevent disuse atrophy [6,7].

FIGURE 1. MG-BASED RING FOR ACL REPAIR

To this end, we have developed a bioresorbable magnesium (Mg)-based ring (Fig. 1) that could bridge the ends of an injured ACL in order to load the insertion sites and provide joint stability [8]. Tests using a robotics/UFS testing system showed that Mg-based ring repair could restore both joint kinematics and in-situ forces close to normal in a cadaveric goat stifle joint [9]. However, the question remained whether Mg-based ring repair could maintain this stability and resist residual elongation under repetitive loading. In addition, we were interested in determining potential sites of elongation such as the tissue ring interface, femoral fixation, or tibial fixation (Fig. 2).

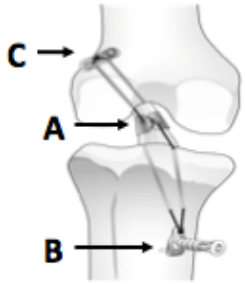

FIGURE 2. POTENTIAL SITES OF RESIDUAL ELONGATION; A-TISSUE-RING INTERFACE, B-FEMORAL FIXATION, AND C-TIBIAL FIXATION

OBJECTIVE

The objective of this study was to perform a cyclic creep test on the Mg-based ring repaired FATC to determine the amount of residual elongation that occurs. In addition, testing of isolated components of the ring procedure was performed to determine the location of any residual elongation.

MATERIALS AND METHODS

Mg-based ring repair of eight (8) cadaveric goat stifle joints was performed using a novel technique [8]. The ACL was first exposed via a medial arthrotomy and transected in its midsubstance. Two 1.5 mm wide bone tunnels were drilled in both the femur and tibia with the femoral tunnels both placed anterior to the ACL insertion site and one tibial tunnel placed laterally with the other placed medially to the ACL insertion site. Two sets of *repair sutures* (Fig. 3) were passed through the ACL tissue before being threaded through the ring. Two sets of *fixation sutures* were also passed through each ACL stump before being passed through suture holes on the ring. The repair sutures were then tied under tension over the suture notches on the ring and the fixation sutures were passed through the opposite bone tunnels and secured in place. Femoral fixation was accomplished using an Endobutton and tibial fixation was accomplished with a double-spiked plate and post (Smith & Nephew, Andover, MA) (Fig. 3).

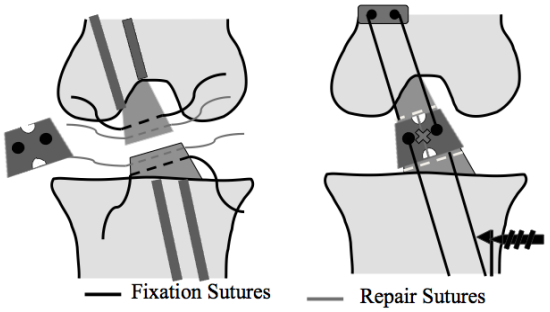

FIGURE 3. SCHEMATIC OF MG-BASED RING

All of the surrounding soft tissues were then removed from the stifle joint to leave only the Mg-based ring repaired FATC. The medial femoral condyle was also removed so the ACL could be aligned uniaxially. The FATC was then mounted in a uniaxial materials testing machine (Instron Model #4502, Norwood MA) and preloaded by 3 N, setting the initial gauge length (GL, Fig. 4). 3 cyclic loading tests were then performed (C1-C3) with 100 cycles each between 20 and 70 N at an elongation rate of 50 mm/min per test [10]. The FATC was allowed to rest for an hour between each testing cycle. After each rest period, the FATC was preloaded and the displacement was recorded (E1, E2, and E3]. Residual elongation was calculated as the difference between E1, E2, or E3 and the initial gauge length (GL).

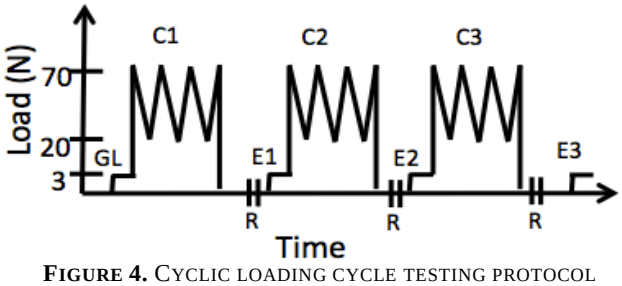

FIGURE 4. CYCLIC LOADING CYCLE TESTING PROTOCOL

Following testing of the Mg-based ring-repaired ACL, individual components of the repair procedure were tested on new goat stifle joints (N=4) to determine the location of residual elongation: the femoral fixation, tibial fixation, and tissue-ring interface. A similar testing procedure was used with the individual components being loaded between 1 and 3 mm which corresponded to the elongation of the entire Mg-based ring repaired FATC at 20 and 70 N. In addition, the gauge length was reset to 0 mm after each preload to ensure that the specimen were still being elongated since the residual elongation could exceed the 1 mm limit.

A repeated measures ANOVA with a post-hoc Bonferroni analysis was used to determine statistical significance between residual elongation values. ($p<0.05$).

RESULTS

Mg-based Ring Repair

TABLE 1. RESIDUAL ELONGATION (MM) OF THE MG-BASED RING REPAIRED FATC. * STATISTICAL SIGNIFICANCE ($P<0.05$).

	Residual Elongation (mm)		
Test Group	**E1**	**E2**	**E3**
Mg-based ring-repaired FATC	1.8±0.8*	2.2±0.2	2.6±0.6*

The results of the cyclic loading tests of the Mg-based ring repaired FATC are shown in Table 1. The total residual elongation after all three loading cycles was 2.6±0.6 mm. The majority of residual elongation occurred at E1 (1.8±0.8 mm, or 66% of the total). Residual elongation increased by 0.4 mm for both E2 and E3.

Isolated Components of Mg-based Ring Repair

TABLE 2. RESIDUAL ELONGATION (MM) OF THE TISSUE-RING INTERFACE, FEMORAL FIXATION, AND TIBIAL FIXATION. * STATISTICAL SIGNIFICANCE ($P<0.05$).

	Residual Elongation (mm)		
Test Group	**E1**	**E2**	**E3**
Tissue-Ring Interface	1.2±0.8	2.0±1.4	2.6±1.6
Femoral Fixation	1.1±0.4	1.7±0.9	1.9±0.8*
Tibial Fixation	1.2±0.5	2.1±0.6	2.4±0.5*

The results of the cyclic loading tests of the isolated components of Mg-based ring repair are shown in Table 2. All three components had similar total residual elongations at E3 with the maximum residual elongation 2.6±1.6 mm occurring at the tissue-ring interface. The increase in residual elongation from E2 to E3 for both the femoral and tibial fixations was the only significant increase in residual elongation ($p<0.05$).

DISCUSSION

The study successfully determined that residual elongation does occur in an Mg-based ring repaired FATC. In addition, the study determined that residual elongation occurs throughout the Mg-based ring repaired FATC. The reason that the amount of residual elongation occurring in the components did not sum to measured residual elongation in the Mg-based ring repaired FATC was likely due to the difference in testing procedures. By resetting the gauge length after each preload for the individual components, the load carried in each component was probably increased above the 70 N used to test the entire Mg-based ring repaired FATC. However, despite this difference the results from the cyclic testing of the individual components still demonstrates that residual elongation is occurring throughout the Mg-based ring repaired FATC.

The observed residual elongation in the Mg-based ring repaired FATC was higher than that obtained previously for a bone-patellar tendon-bone autograft (1.3±0.6 mm) [10]. However, this difference may not be clinically significant and needs to be investigated *in vivo*. In addition, since we have identified that residual elongation occurs throughout the Mg-based ring repaired FATC we can explore design modifications to reduce the amount of residual elongation occurring; for example, we could explore using alternate fixation devices.

Future work on the ring repair procedure will also determine if residual elongation plateaus following additional loading cycles, i.e. C4 and beyond. Finally, the results of these studies could aid in improving knee function following Mg-based ring repair of the ACL and result in positive outcomes during an *in vivo* study to determine the effect of Mg-based ring repair combined with biological augmentation on ACL healing.

CONCLUSIONS

This study demonstrated that residual elongation occurs throughout the Mg-based ring repaired FATC. With this knowledge, we can now optimize the design to minimize residual elongation which should lead to good outcomes *in vivo*.

ACKNOWLEDGEMENTS

The authors gratefully acknowledge the National Science Foundation Engineering Research Center for Revolutionizing Metallic Biomaterials (grant #0812348) and the University of Pittsburgh Honors College Brackenridge Summer Research Fellowship for providing financial support.

REFERENCES

1. Von Porat, et al. 2004. *Ann Rheum Dis*, 63:269-73
2. Salmon, et al. 2006. *J Sports med*, 34:721-32
3. Agung, et al. 2006. *KSSTA*, 14(12):1307-1314
4. Murray, et al. 2006. *JOR*, 24(4):820-830
5. Fisher, et al. 2012. *KSSTA*, 20:1357-1365
6. Fleming, et al. 2008. *JOR*, 26(11):1500-1505
7. Fisher, et al. 2011. *J Biomech*, 44(8):1530-1535
8. Farraro, et al. 2013. McGowan Institute for Regenerative Medicine Annual Retreat.
9. Farraro, et al. 2013. 2013 BMES Annual Meeting
10. Musahl, et al. 2003. *KSSTA*, 11(2) 68-74

Chun-Ho Ma

The Chinese University of Hong Kong

Major: Biomedical Engineering

Junior

S1155015351@cuhk.edu.hk

Lab Mentor: Kwang Kim, B.S.

Faculty Advisor: Savio L-Y. Woo, Ph.D., D. Sc., D. Eng.

I was born April 13, 1992. I live in Hong Kong with my parents and elder sister and brother. My father is a construction worker and my mother is a housewife. I had my secondary education in Munsang College and graduated in 2011. Thanks to my teachers, I have developed interest in biology and mathematics. I chose mathematics stream in my secondary study. Besides, I participated Prefect Association as a committee member, I gained responsibility and have organized various activities for the schoolmates. Outside of school, I joined different social services. I gained communication skill through interaction with different people and learned to be more mature.

I chose the Biomedical Engineering degree programme at the Chinese University of Hong Kong. I acquired the knowledge of biomedical and engineering and learned how to apply theoretical science, that learned in the lessons, into real life. I served as a vice-president of Biomedical Engineering Society, CUHK. I communicated with different societies and organized joint-universities activities for our classmates, so that students from different universities can communicate and exchange information about the biomedical engineering filed. Last summer, I also helped to organize orientation camp for my own college and Engineering Faculty. It is the most memorable to me.

It was my first time to do a research project and work in a lab. I only had basic knowledge about the rotator cuff and suture anchor before working at the MSRC. I got a deeper understanding about the importance of suture anchor in rotator cuff repairing after doing the project on Magnesium-based suture anchor. I not only learned how to conduct mechanical test, but also learned how to plan and design experiment. This was a valuable experience for me.

I would like to thank Dr. Woo for providing this golden opportunity for me to work at MSRC and sharing his experience. His word of wisdom really inspired me a lot. I would also like to thank my mentor Mr. Kim for his guidance and teaching me to become more independent.

TENSILE TESTING OF A MAGNESIUM-BASED SUTURE ANCHOR

Chun Ho Ma, Kwang Kim, B.S., Savio L-Y. Woo, Ph.D., D.Sc., D.Eng.

Musculoskeletal Research Center, Department of Bioengineering, University of Pittsburgh

INTRODUCTION

Suture anchors are commonly used in repairing and reconstruction of soft tissue in musculoskeletal system. For example, rotator cuff repairing and arthroscopic repair of a torn acetabular labrum [1]. Approximately 300,000 surgeries are performed in the US to repair rotator cuff tears each year [2]. Typically, 2 to 4 suture anchors are used for repairing the torn end of the tender of humeral head in many rotator cuff repair surgeries [3, 4]. Thus, the number of suture anchors utilized for rotator cuff surgery each year may reach up to one million.

The existing commercial suture anchors are made of either metals, like titanium alloys, or bioresorbable polymers, such as PLLA. Unfortunately, they suffer from various complications. Metallic suture anchors suffer from complication of revision surgeries, migration or loosening and interference with post-operative MRI [5, 6]. Although bioresorbable polymer-based suture anchors were developed to overcome these shortcomings, they may be non-biodegradable, are easy to fracture due to reduced strength, and lead to osteolysis [7, 8].

Studies showed that Magnesium (Mg)-based alloys are biodegradable, possess superior mechanical properties compared to polymers, and promote bone regeneration [9, 10]. We believe that suture anchors made of Mg-based alloys would therefore capture the advantages of both metallic and polymer-based materials, while eliminating their disadvantages. In order to optimize the design of Mg-based suture anchors in consideration of the unique mechanical properties of Mg-based alloys, finite element analysis can be performed prior to manufacturing prototypes for costly in vitro and in vivo animal evaluation.

OBJECTIVE

The objective of this study was to perform a pullout test of a new suture anchor design to obtain the pullout force, displacement at pullout and the mode of failure. The result will be used to validate a finite element model of Mg-based suture anchor.

MATERIALS AND METHODS

Suture anchor plastic prototype, which was 3D printed, was used. The outer diameter was 6 mm, inner diameter was 4.75 mm, length was 16.5 mm and thread pitch was 1.15mm (**Figure 1**).

A hole with diameter 4.75 mm which is the same as the inner diameter of the anchor, was pre-drilled on a precut block (13 cm x 4.5 cm x 4 cm) of a uniformly rigid polyurethane foam (ASTM F-1839-08), (15 pcf, SAWBONES, Vashon, WA). The pre-drilled hole was then tapped. Steel wire, serving in place of a suture to eliminate suture breakage as a possible failure mode, was passed through the distal eyelet of anchor. The anchor was inserted in pre-drilled polyurethane foam. The two ends of steel wire were clamped to form a loop. Tension was applied axially to the suture anchor to stimulate the worst case scenario, therefore, pullout testing was performed at 90 degrees to the surface of the polyurethane foam (**Figure 2**). The set-up was then loaded to failure on a mechanical testing machine, Instron 5565, at an elongation rate 10 mm/minute. The ultimate load and elongation at failure were recorded.

Figure 1 The 3D printed plastic prototype used.

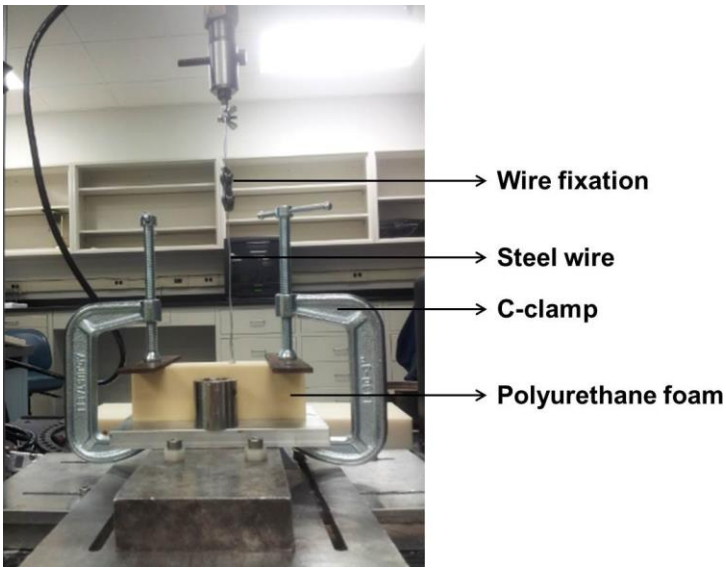

Figure 2 Pull out test setup.

RESULTS

Three pullout tests of plastic suture anchors were performed successfully. Load-displacement curves were obtained (**Figure 3**).

The pullout force of plastic prototype suture anchor was 116.9 ± 13.7 N. The displacement at pullout was 4.0 ± 1.3 mm. The suture anchors were pulled out from the bone block in all cases (**Table 1**).

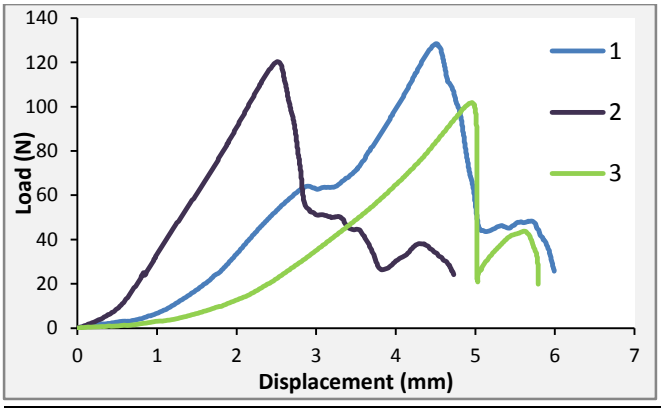

Figure 3 Load-displacement curve obtained from three pullout tests of the plastic suture anchor.

Table 1 Pullout force and displacement at pullout was obtained from the load-displacement curve.

Pullout Force	116.9 ± 13.7 N
Displacement at pullout	4.0 ± 1.3 mm

DISCUSSION

The objective of this study was to perform a pullout test of a new design of Magnesium (Mg)-based suture anchor to validate a finite element model of the Mg-based suture anchor. Pullout force, displacement at pullout and failure mode were determined. Plastic prototypes were generated via 3D printing and were used to practice the experiment before using actual Mg-based suture anchors.

In previous study, Craig R. Bottoni, et al., found that the mean pullout force of polymer suture anchor and metallic suture anchor were 227.17 N and 176.40 N respectively. The pullout force of plastic suture anchor we found was lower than the value of previous study. It is reasonable because we tapped the pre-drilled hole. This may reduce the pullout force.

We have encountered problems during the experiment. The main issue was that plastic suture anchors were broken while inserting into polyurethane foam. Since it is a novel design, there was no suitable driver for insertion. We used a wrench to turn it. Plastic suture anchor was too weak to withstand the torque generated while turning. Therefore, we decided to tap it before insertion. A steel wire was used because it is strong enough that it will not be broken during pullout test and to make sure that the elongation is at the suture anchor instead of steel wire. But it was difficult to make sure that the steel wire was straight before performing the pullout test. Because steel wire was passed through the eyelet before insertion and it was bended. Time and force were used to straighten the steel wire. Therefore, pullout force obtained was not accurate and the actual pullout force should be lower than that we obtained from the pullout test.

Main limitation of this study was that the plastic suture anchor was generated via 3D printing. The edge of the thread was not sharp, it made difficult to insert the suture anchor. But we believe that the real Mg-based suture anchor will not have this problem. Moreover, since we could not insert the suture anchor, we tapped the pre-drilled hole. But the tap we used was not identical to the thread size of the anchor. We used a tap which is larger than the anchor. This may had reduced the pull-out force.

Although the finding was not satisfying, it is good to use a plastic prototype to practice before using real Mg-based suture anchor. It can show what design modifications are needed to be made to make a better suture anchor and easier to insert into the polyurethane foam. We decided to reduce the number of thread, since it is inconvenient to a surgeon to do operation if too many turns are required. In actual testing, braided steel wire should be used, which is more flexible, instead of steel to ensure that it is straight at the beginning of the testing.

A finite element model of suture anchor will be made to predict pullout force. The pullout force obtained experimentally will then be compared with the predicted pullout force in the model. If two values are closed enough, this means that the model can predict the pullout force accurately and we then can use the model to predict pullout force of suture anchors with different design. Thus, which design gives the strongest pullout force can be found.

REFERENCES

1. M.J. Philippon, S.P. Arnoczky, and A. Torrie, Arthroscopy. 23(4): p. 376-80. 2007.
2. A.C. Colvin, et al., J Bone Joint Surg Am. 94(3): p. 227-33. 2012.
3. C.B. Ma, et al., Journal of Bone and Joint Surgery-American Volume. 88A(2): p. 403-410. 2006.
4. M. Ozbaydar, et al., Journal of Bone and Joint Surgery-British Volume. 90B(10): p. 1386-1391. 2008.
5. L.W. Bancroft, et al., Magn Reson Imaging Clin N Am. 20(2): p. 313-25, xi. 2012.
6. Craig R, et al., 2008. Orthopedics, Volume 31 · Issue 11:
7. A. Dhawan, et al., Am J Sports Med. 40(6): p. 1424-30. 2012.
8. M. Muller, et al., Injury-International Journal of the Care of the Injured. 33: p. 30-36. 2002.
9. F. Witte, et al., J Biomed Mater Res A. 81(3): p. 757-65. 2007.
10. Peng Q, et al., 2013. Degradable magnesium-based implant materials with anti-inflammatory activity. J Biomed Mater Res Part A 2013:101A:1898–1906

Sara Orr

Pennsylvania State University

Major: Bioengineering

Junior

sao5122@psu.edu

Lab Mentor: Jonquil Flowers, B.S., M.S.

Faculty Advisor: Savio L-Y. Woo, Ph.D., D. Sc., D. Eng.

I was born on January, 19th 1993 and grew up an hour east of Pittsburgh in Greensburg, PA. In 2011, I graduated from Greensburg Salem High School, where I earned nine varsity letters in cross country, swim team, softball, and lacrosse. I also enjoyed being treasurer of the American Red Cross Club, president of the Students Helping Other People Club, an executive officer of the National Honors Society, and captain of the cross country team. Outside of school, I enjoyed playing the violin and kiteboarding in my free time. During my summers, I worked in the family business, a precision machine products company. My experience in my family's business, as well as my interest in math and biology, led me to pursue a degree in bioengineering.

I am going to be a junior in the Schreyer Honors College at Pennsylvania State University. I am majoring in bioengineering with an option in materials science. When I am not busy with school work, I enjoy being an active member of the Penn State community. I am a member of Penn State Women in Engineering and the Engineering Leadership Societies. I love being involved in THON, the Penn State Dance Marathon that is the largest student-run philanthropy in the world. I have been on a Morale Committee and participate in the THON Organization Apollo. I have also had two amazing international experiences through Penn State. My freshman year, I travelled to Ghana with the Global Medical Brigades and worked in a medical clinic. Spring semester of my sophomore year, I studied abroad in Florence, Italy. I look forward to making the most of the rest of my time at Penn State.

I applied for the Summer Undergraduate Research Program at the MSRC after looking into a variety of possible research positions for the summer. The MSRC captured my attention because I am interested in functional tissue engineering and tissue regeneration for my honors thesis and for my future career as a bioengineer. I also had an ACL reconstruction last summer, so I have a more personal interest in the MSRC's work. Previously, I had no research experience, but I have learned so much thanks to my summer at the MSRC. I have learned about the research process in general and, more specifically, about ACL reconstruction and bioscaffolds. I would like to thank Dr. Woo for sharing his expertise and providing me with guidance. I would also like to thank my mentor, Jonquil Flowers, for her support and advice, as well as Katie Farraro, Kwang Kim, and Dr. Zhang for their leadership this summer.

THE QUANTIFICATION AND COMPARISON OF GROWTH FACTOR, SOLUBLE COLLAGEN, AND SULFATED GLYCOSAMINOGLYCAN CONTENT IN SIS AND UBM HYDROGELS

Sara Orr, Cuiling Zhang, M.D, Ph.D., Jonquil Flowers, M.S., Katie Farraro, M.S., Kwang Kim, B.S., Savio L-Y. Woo, Ph.D., D.Sc., D.Eng.
Musculoskeletal Research Center, Department of Bioengineering, University of Pittsburgh

INTRODUCTION

Extracellular matrix (ECM) bioscaffolds derived from mammalian tissues have been used to successfully regenerate a variety of injured tissues, including ligaments and tendons [1,2,3,4]. Of these ECM bioscaffolds, small intestinal submucosa (SIS) and urinary bladder matrix (UBM) bioscaffolds have been studied most comprehensively [5].

SIS and UBM bioscaffolds are first prepared in a sheet form known to retain collagen, glycosaminogylcans (GAGs), and growth factors, most abundantly FGF-2 and TGF- β1, from the native tissues from which they are derived [6,7,8,9]. However, they can also be further processed into a hydrogel by milling the sheets into powder, performing a pepsin digest, and bringing the temperature and pH to physiological levels. Hydrogels are particularly desirable because they could potentially mold to any shape and be injected in minimally invasive procedures [5]. While ECM hydrogels have been shown to have beneficial effects on healing tissues [4,10,11], the mechanisms behind these effects are not fully understood. Further characterization of these gels is needed to explore if they retain these structural and functional molecules after pepsin digestion. Identifying and quantifying the presence of these structural and functional molecules could lead to a better understanding of the beneficial effects of ECM hydrogels.

OBJECTIVE

The objective of this study was to identify, quantify, and compare the content of FGF-2, TGF-β1, soluble collagen, and sulfated GAG in porcine SIS and UBM hydrogels.

We hypothesized that FGF-2 and TGF-β1 would be present in both SIS and UBM hydrogels, but in lesser amounts than in the sheet forms due to the pepsin digestion. We also hypothesized that soluble collagen and sulfated GAGs would be present in similar amounts in SIS and UBM hydrogels.

MATERIALS AND METHODS

Preparation of SIS and UBM Hydrogels

SIS and UBM pre-gel pepsin digests were provided by our collaborator. Their preparation has been previously described [5,6,7,11]. In brief, lyophilized powder from SIS and UBM sheets was digested in a solution of 1 mg/ml porcine pepsin in 0.01 N HCl to a 10 mg ECM/ml (dry wt.) content. This form is known as the pre-gel pepsin digest (Figure 1). To induce gelation, the pH is neutralized and the pre-gel pepsin digest is warmed to 37 °C.

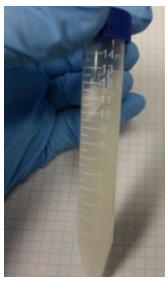

Figure 1: Pepsin digest of SIS before gelation

Growth Factor Content

Enzyme-linked immunosorbent assays (ELISA) were used to quantify the presence of FGF-2 and TGF-β1 in SIS and UBM pre-gel pepsin digests. To prepare the samples for the FGF-2 ELISA (Human FGF

basic Quantikine ELISA Kit DBF50, R&D Systems), the pre-gel pepsin digest forms of SIS and UBM were diluted 1:1 with deionized water. For the TGF-β1 ELISA (Human TGF-beta 1 Quantikine ELISA kit DB100B, R&D Systems), collagenase was added to DMEM, which was then added to SIS and UBM pre-gel pepsin digests in a 1:1 ratio. The samples were brought to a pH of 7.4 with 0.1 N NaOH and then incubated at 37 °C overnight. Then, the samples were lyophilized for 24 hours and reconstituted with RD5-53 (1X), a buffer provided in the TGF-β1 ELISA kit. The ELISAs were then completed per the manufacturer's instructions (n = 4). The optical densities were determined using a microplate reader with a wavelength of 450 nm and a reference wavelength of 570 nm. A pepsin buffer was used in both ELISAs as a negative control.

Soluble Collagen Content

The soluble collagen content of the SIS and UBM pre-gel pepsin digests was determined using the Sircol Soluble Collagen Assay (Biocolor Ltd., Carrickfergus, United Kingdom). The SIS and UBM pre-gel pepsin digests were neutralized with 10X PBS and 0.1 N NaOH prior to the assay and also diluted with 1X PBS. A pepsin buffer was used as a negative control. The assay was preformed per the manufacturer's instructions (n = 3). The optical density was determined using a microplate reader with a wavelength of 555 nm.

Sulfated GAG Content

The sulfated GAG content of SIS and UBM pre-gel pepsin digests was determined using the Blyscan Sulfated Glycosaminoglycan Assay (Biocolor Ltd., Carrickfergus, United Kingdom). The SIS and UBM pre-gel pepsin digests were neutralized with 10X PBS and 0.1 N NaOH prior to the assay. A pepsin buffer was tested as a negative control. The assay was preformed per the manufacturer's instructions (n = 3). The optical density was determined using a microplate reader with a wavelength of 656 nm.

Statistical Analysis

Student's t-tests were used to analyze the FGF-2, TGF-β1, soluble collagen, and sulfated GAG content of the SIS and UBM pre-gel pepsin digests. Significance was defined as $p < 0.05$.

RESULTS

Growth Factor Content

Table 1 shows the FGF-2 and TGF-β1 content of SIS and UBM pre-gel pepsin digests. For both growth factors, the differences in quantities between the pre-gel digests were not statistically significant ($p > 0.05$).

Soluble Collagen Content

Table 1 shows the soluble collagen contents of SIS and UBM pre-gel pepsin digests. It was found that the UBM digest contained 2.7 times the amount of collagen of the SIS digest, and the difference was statistically significant ($p < 0.05$).

Sulfated GAG Content

Table 1 shows the sulfated GAG content of SIS and UBM pre-gel pepsin digests. The difference between the values for SIS and UBM pre-gel pepsin digests was not statistically significant ($p > 0.05$).

Table 1. The growth factor, soluble collagen, and sulfated GAG content of SIS and UBM pre-gel pepsin digests (mean ± SD). * denotes statistical significance between the two ECM types.

	SIS	UBM
FGF-2 Content (ng g^{-1} dry ECM powder)	81 ± 36	51 ± 12
TGF-β1 Content (ng g^{-1} dry ECM powder)	4.4 ± 0.6	4.6 ± 0.6
Soluble Collagen Content (mg mg^{-1} dry ECM powder)	0.38 ± 0.04*	1.02 ± 0.10*
Sulfated GAG Content (μg mg^{-1} dry ECM powder)	2.34 ± 1.17	1.77 ± 1.37

DISCUSSION

The objective of this study was to identify, quantify, and compare the content of FGF-2, TGF-β1, soluble collagen, and sulfated GAG in porcine SIS and UBM hydrogels. FGF-2 and TGF-β1 were indeed found

to be present in both SIS and UBM pre-gel pepsin digests. FGF-2 was present in similar quantities to those reported in SIS and UBM sheet forms [8]. However, TGF-β1 was found in much lower quantities in the pre-gel pepsin digests than what has been found in the sheet forms, about one-tenth of the amount [8]. This suggests that the pepsin digestion may affect these proteins differently. These results partially confirmed our hypothesis that the growth factors would be present in lesser amounts in the hydrogels than in the sheet forms.

Soluble collagen was found in similar amounts in UBM pre-gel pepsin digests as to what has been found in previous studies [6,7]. There was a statistically significant difference between the soluble collagen content of SIS and UBM pre-gel pepsin digests, with the UBM pre-gel pepsin digest containing more soluble collagen. This did not confirm our hypothesis that SIS and UBM hydrogels would contain similar amounts of soluble collagen.

The sulfated GAG content was found to be variable between different batches of SIS and UBM, resulting in large standard deviations. For the UBM, the sulfated GAG content was lower than what previous studies have found [6,7]. Our hypothesis that SIS and UBM hydrogels would contain similar amounts of sulfated GAGs was confirmed, as the difference in GAG content between the two pre-gel pepsin digests was not statistically significant. However, further investigation into the GAG content of SIS and UBM pre-gel pepsin digests is warranted. It is possible that the methods need to be refined or that a papain extraction should be performed prior to the assay.

Future studies should determine if the growth factors are present in a bioactive form in the SIS and UBM hydrogels. To do this, a cell proliferation assay to evaluate the effects of protein extracts from SIS and UBM hydrogels could be performed. Additionally, there are other functional and structural molecules that should be quantified and compared, such as laminin, fibronectin, glycoproteins, and proteoglycans. These studies would lead to a better understanding of the role that functional and structural components play in the beneficial effects that ECM hydrogels have on healing tissues.

CONCLUSIONS

ECM hydrogels have great potential to aid in the repair and reconstruction of healing tissues. This study has contributed findings that may suggest why SIS and UBM hydrogels have these beneficial effects on healing tissues. It also suggests that different ECM hydrogel types may have distinct properties that could affect which ECM type should be used in certain applications.

ACKNOWLEDGEMENTS

We would like to thank Dr. Stephen F. Badylak for supplying the pre-gel pepsin digests of SIS and UBM.

REFERENCES

11. Cartmell JS, et al, *J BIomen Mater Res* 2000;49:134-40
12. Woods T, et al, *PF. Biomaterials* 2005;26(35):7339-49, Dec.
13. Liang R., et al, *J Orthop Res*, 2008, 28(8):1098-104
14. Fisher MB., et al, *Knee Surg Sports Traumatol Arthrosc*, 2012 Jul:20(7):1357-65
15. Badylak SF., et al, *Acta Biomater*, 2009 Jan:5(1):1-13
16. Freytes DO., et al, *Biomaterials*, 2008 Apr:29(11):1630-7
17. Wolf MT., et al, *Biomaterials*, 2012 Oct:33(29):7028-38
18. Liang R., et al, *Acta Biomater*, 2011 Apr:7(4):1719-27
19. Badylak S.F., *Semin Cell Dev Biol*, 2002:13(5):377-383
20. Badylak S.F., et al, *Transpl Immunol*, 2004:12(3-4):367-377
21. Badylak, S.F., et al, *Anat Rec B New Anat*, 2005:287(1):36-41

Ashley Smoots

University of Pittsburgh

Bioengineering

ans155@pitt.edu

Lab mentor: Bill Barone

Faculty advisor: Steve Abramowitch

Ashley grew up outside of Philadelphia in Yardley, Pennsylvania. During college she has been very active throughout the engineering school, serving as an engineering ambassador and holding multiple offices within the school's chapter of National Society of Black Engineers. After graduation, she plans to pursue a master's degree. Ashley really enjoyed working in the lab this summer and learning new skills as she conducted her research.

DEVELOPMENT OF A CRYOGEN FREEZING PROTOCOL FOR SOFT TISSUES

Ashley Smoots[1], William Barone[1], Pamela A. Moalli[2] MD, PhD, Steven Abramowitch[1,2] PhD
[1]Musculoskeletal Research Center, Department of Bioengineering, University of Pittsburgh.
[2]Urogynecology & Reconstructive Pelvic Surgery, Magee-Women's Hospital, University of Pittsburgh

INTRODUCTION

Pelvic organ prolapse (POP) is a pelvic floor disorder in which the pelvic organ are no longer supported properly. This results in a descent of the pelvic organs causing them to push against the vagina. While the majority of the women suffering this condition are 65 years or older, as the population ages, the prevalence of POP will increase as well. Current therapies for pelvic organ prolapse include the use of a synthetic mesh. The mesh is inserted surgically and acts as a sling to provide support for the pelvic organs and restore the anatomy of the vagina (Gomelsky et al, 2011). In general, surfaces will erode softer surfaces when they come in contact. This concept in applicable to vaginal mesh, and a surgical complication of mesh repair for prolapse that meshes are eroding the tissue upon implantation (Afonso et al, 2008). Though tissue erosion is associated with synthetic implants, they are still used in vivo for tissue repair and reinforcement (Dietz et al, 2003), and currently up to 20% of all mesh surgeries will require a repeat operation (Bako et al, 2009).

The Food and Drug Administration (FDA) do not closely monitor synthetic meshes used for pelvic organ prolapse repair because they resemble the approved meshes used for hernia repair. In 2008 the FDA released a public health warning about vaginal mesh use due to a high prevalence of complications. Previous studies support the use of polypropylene mesh in POP repair, however mesh erosion remains a prevalent unsolved complication (Afonso et al, 2008).

It has been shown that in tissue samples that undergo cryofixation as opposed to other freezing methods, such as liquid nitrogen fixation in O.C.T., have enhanced immunoreactivity in comparison to other methods and do not require additional pretreatments (Ohno, 2004). By following a cryofixation protocol there is a reduction in image-altering effects that are attributed to ice crystal formation in samples. This reduction will likely expose the samples' inherent morphological characteristics. It has been found that in in-vivo cryo-frozen samples, blood flow is preserved and displayed with directivity. In pathological samples it has been shown that in-vivo cryo-freezing prevents the morphological changes that occur when using older collection techniques (Shi, 2012).

OBJECTIVE

The objective of this project is to develop a protocol for the quick freezing of tissues using isopentane cryogen. Once the protocol is established, it will be used to determine if it's possible to isolate specific portions of the tissue for analysis. We will also compare the images obtained of tissues frozen in the traditional method and the cryogen fixation method. This comparison will demonstrate whether the new protocol results in less ice crystal formation during the freezing process.

METHODS

Isopentane cryogen was produced by combining liquid isopentane (2-methylbutane, Fisher Scientific, Fair Lawn NJ) and ultra high purity propane gas (99.99%, Matheson Inc, Basking Ridge NJ) at a 1:2 ratio. Figure 1 demonstrates the setup used for cryogen production. The isopentane cryogen is produced by suspending a beaker in a Styrofoam box, submerging the bottom of the beaker in liquid nitrogen. This Styrofoam box is positioned on a stir plate such that a stir bar can be used in the beaker to facilitate the reaction. Isopentane is frozen in the beaker by the liquid nitrogen in the container, and when it has solidified high purity propane is blown into the beaker and combined with the isopentane.

Figure 1. Image of the cryogen production apparatus. A beaker is suspended in a Styrofoam box by wire. High purity propane is blown directly into the beaker to produce isopentane cryogen.

The samples frozen by the traditional method were placed in O.C.T. (Optimum Cutting Temperature, Tissue-Tek) and then frozen with the O.C.T. over liquid nitrogen (-196°C). The samples prepared by cryogen fixation were frozen directly in the isopentane cryogen (-193°C) and then transferred to liquid nitrogen for further freezing. The samples were removed from the liquid nitrogen, then placed into O.C.T. and frozen with the O.C.T. over liquid nitrogen in the same manner as the traditionally prepared samples. When the drilling of a tissue to obtain a specific sample was required, it was done after removal from the liquid nitrogen and only the extracted sample was frozen in the O.C.T.

The freezing protocols were carried out on previously dissected vaginal samples as well as freshly dissected hearts and kidneys. The vaginal samples were frozen with the cryogen protocol and then ½" samples were drilled out using a ½" diamond coated drill saw and a Dremel 4000. The rats were dissected and one heart and two kidneys were procured from each animal. Each of the hearts was frozen in a different method, either by cryo-fixing or the traditional method. Each of the kidneys procured from each animal were prepared by different protocols. All of the O.C.T. blocks were cut on a cryostat to create 7-micrometer thick slides. The slides were stained with a Hemotoxylin and Eosin stain as well as Masson's Trichrome staining.

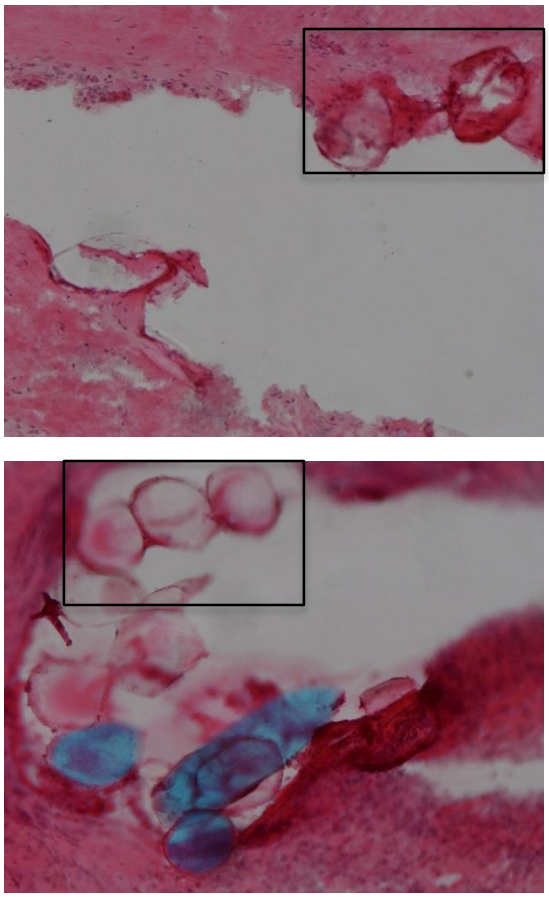

Figure 2. Hemotoxylin and eosin stain of human vagina mesh. The upper image shows the mesh in a sample of tissue that was frozen using the cryogen freezing protocol and the lower image shows mesh in a traditionally frozen tissue sample.

RESULTS/DISCUSSION

We found that tissues froze quickly in the cryogen, to a state that can be described as 'as hard as a tooth'. In the human vaginal tissue, it was possible to drill out samples using the Dremel 4000 and to freeze these samples in the O.C.T. for slide preparation. These slides do not show negative effects on the edges from the use of the drill.

In the human vaginal tissues it is possible to see the mesh in the cryogen frozen samples just as clearly as it can be seen in a traditionally fixed sample of the same tissue (Figure 2). The vaginal tissue sample was frozen at -80°C prior to the use of cryogen fixation; therefore the integrity of the structures within the tissue sample is unable to provide evidence that the cryogen fixation protocol is or is not effective.

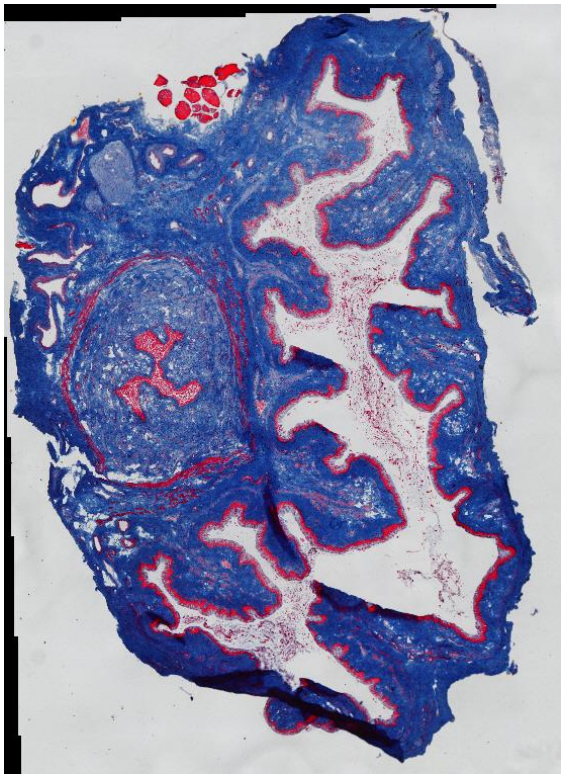

Figure 3. Masson's Trichrome stain of rat vagina. The urethra can be seen clearly, stained red within a blue circle. The vagina is represented by the large, mostly white space on the right of the structure.

The cryogen freezing process was also performed on previously frozen rat vaginas (Figure 3). In these samples you are able to see the vagina and urethra, and there are again no negative edge effects as a result of the drill. The lack of edge effects supports this method for use in the isolation of specific tissue regions.

In the rat cardiac tissue, the cryogen-frozen samples have a spongy appearance, and show no other structure. This is a freezing artifact and should not occur naturally within the tissue.

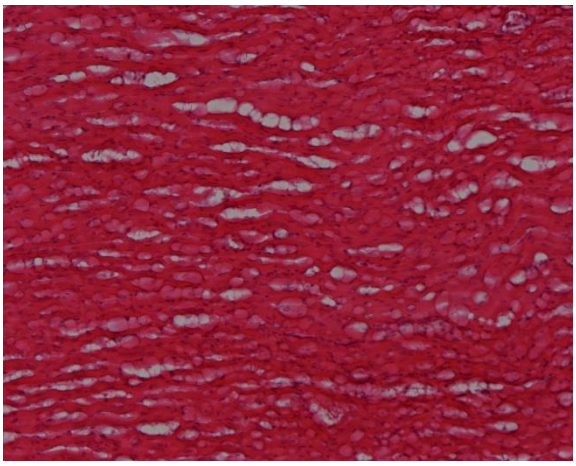

Figure 4. Hemotoxylin and eosin stain of cryogen frozen rat heart. The cryogen frozen cardiac muscle has a sponge like appearance.

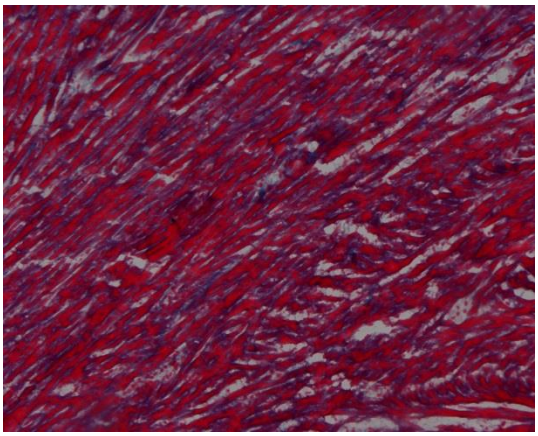

Figure 5. Hemotoxylin and eosin stain of traditionally frozen rat heart. The traditionally frozen cardiac muscle does not exhibit much structure.

The traditionally frozen cardiac tissue does not show the sponge-like artifact nor does it maintain its full structure. There are not distinct red blood cells visible in the sample, which can likely be attributed to the slow freezing time of the traditional fixation method, which takes 2 minutes and 20 seconds.

Blood vessels can be seen in tissue samples frozen by both methods. While the vessels in the tissue frozen by the traditional method appear flat, those in tissue frozen by the cryogen freezing protocol have a tubular, three dimensional appearance. The traditional method of freezing is slow, which likely allows time for blood vessels to collapse prior to fixation.

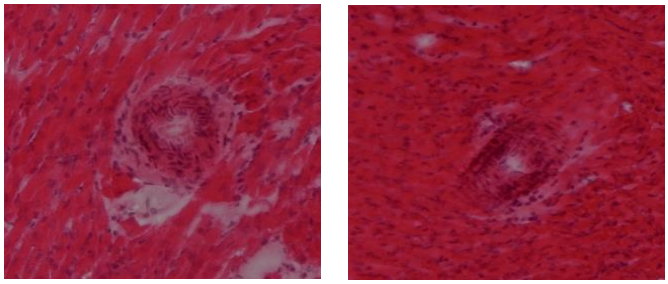

Figure 6. Blood vessels in rat heart. The traditionally frozen blood vessel (left) and the cryogen frozen blood vessel (right) display differences in appearance, the cryofixed vessel appears to be tubular.

In the kidney tissue, the distal tubules are seen in samples prepared by both methods. At the same magnification, the tubules appear larger in the traditionally fixed sample than in the cryogen frozen sample.

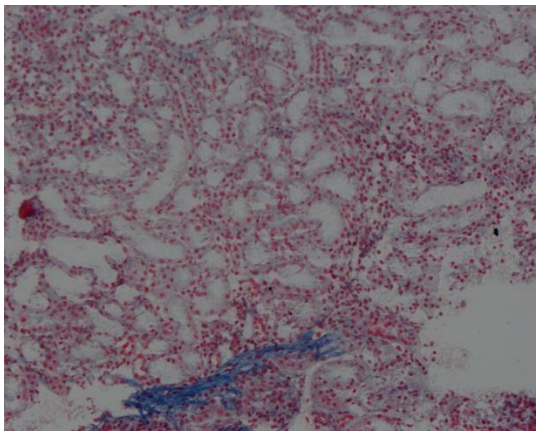

Figure 7. Masson's trichrome stain of traditionally frozen kidney. The distal tubules of the kidney can be seen clearly in the traditionally frozen sample.

The difference in size between the tubules is likely due to either ice crystal formation in the traditionally frozen sample causing distortions in the tissue or significant differences in between the natural size of each of the kidneys.

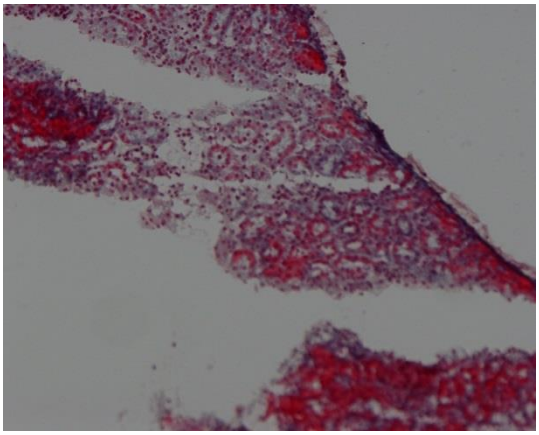

Figure 8. Masson's trichrome stain of cryo-frozen rat kidney. The distal tubules can be seen the cryogen frozen kidney, though they appear small.

LIMITATIONS

The limitations of these results are important to consider. The vaginal tissue used was previously stored at -80 °C and was thawed for use in the cryogen fixation protocol. Because of the multiple freezings of the tissue, the structural integrity post cryo-fixation, which is being examined, is not an accurate tool for determining the success of the cryogen fixation protocol in reducing freezing artifacts. When comparing the structure of rat organs frozen by both methods, different organs were used and therefore there cannot be a direct comparison between the appearance of structures present in the tissue, as differences may be a result of the freezing method used or differences in the tissues themselves.

CONCLUSION

This preliminary work shows that the cryogen fixation method can be used to obtain histological results of tissue, and that samples of tissue can be isolated for independent study.

FUTURE WORK

The next steps in determining the effectiveness of the cryo-fixation protocol is to perform a freezing method comparison on additional animals. By preparing halves of same organ in each method, effects of the freezing protocol can be directly compared. It’s also important to

our research to identify effects of cryo-freezing on vaginal structure, as that is the tissue most frequently used. In the long term, we would like to perform biochemical assays on the samples, as well as cryo-freeze the vagina-mesh-bone as single complex.

ACKNOWLEDGEMENTS

This project was made possible through the guidance and support of the Pre-Ph.D. Summer Engineering Research Experience program, under the leadership of Dr. Sylvanus Wosu. I would not have been able to successfully complete this project without the guidance of my mentors Bill Barone and Dr. Steve Abramowitch. I would also like to thank Stacy Palcsey and Alexis Nolfi for teaching me the histology used in this project.

REFERENCES

[1] Abramowitch, S. D., Feola, A., Jallah, Z., & Moalli, P. A. (2009). Tissue mechanics, animal models, and pelvic organ prolapse: a review. European Journal of Obstetrics & Gynecology and Reproductive Biology, 144, S146-S158.

[2] Afonso, JS, Martins, PALS, Girao, MJBC, Jorge, RM Natal, Ferreira, AJM, Mascarenhas, T, . . . de Lima, G Rodrigues. (2008). Mechanical properties of polypropylene mesh used in pelvic floor repair. International Urogynecology Journal, 19(3), 375-380.

[3] Bako, A., & Dhar, R. (2009). Review of synthetic mesh-related complications in pelvic floor reconstructive surgery. International Urogynecology Journal, 20(1), 103-111.

[4] Barber, Matthew D, Brubaker, Linda, Nygaard, Ingrid, & Wheeler, Thomas L. (2009). Defining success after surgery for pelvic organ prolapse. Obstetrics and gynecology, 114(3), 600.

[5] Borazjani, Ali, et al. "Animal models of female pelvic organ prolapse: lessons learned." Expert Review of Obstetrics & Gynecology 7.3 (2012): 249+. Academic OneFile. Web. 3 June 2013.

[6] Clavert, P., Kempf, J. F., Bonnomet, F., Boutemy, P., Marcelin, L., & Kahn, J. L. (2001). Effects of freezing/thawing on the biomechanical properties of human tendons. Surgical and Radiologic Anatomy, 23(4), 259-262.

[7] Dietz, H. P., Vancaillie, P., Svehla, M., Walsh, W., Steensma, A. B., & Vancaillie, T. G. (2003). Mechanical properties of urogynecologic implant materials. International Urogynecology Journal, 14(4), 239-243. doi: 10.1007/s00192-003-1041-8

[8] Diwadkar, Gouri B, Barber, Matthew D, Feiner, Benjamin, Maher, Christopher, & Jelovsek, J Eric. (2009). Complication and reoperation rates after apical vaginal prolapse surgical repair: a systematic review. Obstetrics & Gynecology, 113(2, Part 1), 367-373.

[9] Gomelsky, Alex, Penson, David F, & Dmochowski, Roger R. (2011). Pelvic organ prolapse (POP) surgery: the evidence for the repairs. BJU international, 107(11), 1704-1719.

[10] Liang, R., Abramowitch, S., Knight, K., Palcsey, S., Nolfi, A., Feola, A., ... & Moalli, P. A. (2013). Vaginal degeneration following implantation of synthetic mesh with increased stiffness. BJOG: An International Journal of Obstetrics & Gynaecology, 120(2), 233-243.

[11] Moon, D. K., Woo, S. L., Takakura, Y., Gabriel, M. T., & Abramowitch, S. D. (2006). The effects of refreezing on the viscoelastic and tensile properties of ligaments. Journal of biomechanics, 39(6), 1153-1157.

[12] Nygaard, Ingrid E, McCreery, Rebecca, Brubaker, Linda, Connolly, AnnaMarie, Cundiff, Geoff, Weber, Anne M, & Zyczynski, Halina. (2004). Abdominal sacrocolpopexy: a comprehensive review. Obstetrics & Gynecology, 104(4), 805-823.

[13] Ohno, Nobuhiko, Terada, Nobuo, & Ohno, Shinichi. (2004). Advanced application of the in vivo cryotechnique to immunohistochemistry for animal organs. Acta Histochemica et Cytochemica, 37(6), 357-364.

[14] Ohno, Shinichi, et al. "Significance of ‘in vivo cryotechnique’for morphofunctional analyses of living animal organs." Journal of electron microscopy 59.5 (2010): 395-408.

[15] Shepherd, Jonathan P, Feola, Andrew J, Abramowitch, Steven D, & Moalli, Pamela A. (2012). Uniaxial biomechanical properties of seven different vaginally implanted meshes for pelvic organ prolapse. International Urogynecology Journal, 23(5), 613-620.

[16] Shi, Liye, Li, Zilong, Zhai, Xiaoyue, Ning, Bin, Yang, Bei, & Qi, Guoxian. (2012). Application of "In Vivo Cryotechnique" to Morphological and Immunohistochemical Analyses of Living Mouse Subepicardial Microcirculation Under Various Pathological Conditions. Applied Immunohistochem Mol Morphol, 20(3), 304-317.

[17] Sung, Vivian W, Rogers, Rebecca G, Schaffer, Joseph I, Balk, Ethan M, Uhlig, Katrin, Lau, Joseph, . . . Clemons, Jeffrey L. (2008). Graft use in transvaginal pelvic organ prolapse repair: a systematic review. Obstetrics & Gynecology, 112(5), 1131-1142.

[18] Svabík, Kamil, Martan, Alois, Masata, Jaromir, El-Haddad, Rachid, Hubka, Petr, & Pavlikova, Marketa. (2011). Ultrasound appearances after mesh implantation—evidence of mesh contraction or folding? International Urogynecology Journal, 22(5), 529-533

Jennifer Yeager

University of Pittsburgh

Bioengineering

jly24@pitt.edu

Lab Mentors: William Barone and Katrina Knight

Faculty Advisor: Dr. Steven Abramowitch

Jennifer is from Bethlehem, Pennsylvania and is a senior bioengineering student at the University of Pittsburgh. She is also minoring in chemistry and mathematics and is hoping to find a job in industry after graduation this spring.

Since joining the lab as a sophomore, Jennifer has focused on the biaxial testing of highly compliant planar tissues. She worked alongside her mentors to design and fabricate an improved biaxial testing device and to validate the design. Additionally, she is contributing to current studies utilizing the biaxial device and hopes to conduct future research investigating the effects of pregnancy on pelvic organ prolapse.

IMPROVING THE PERFORMANCE OF A BIAXIAL DEVICE TO MECHANICALLY TEST HIGHLY COMPLIANT PLANAR TISSUES

Jennifer Yeager[1], William Barone[1], Pamela A. Moalli[2] MD, PhD, Steven Abramowitch[1,2], PhD

[1]Musculoskeletal Research Center, Department of Bioengineering

[2]Urogynecology & Reconstructive Pelvic Surgery, Magee-Women's Hospital

University of Pittsburgh, PA, USA

Email: jly24@pitt.edu Web: http://www.pitt.edu/~msrc/

INTRODUCTION

Soft tissue biomechanics is an important aspect of clinical and engineering research. Some important tissues being studied include skin, tendons, heart valves, blood vessels, and vaginal tissue.

Soft tissues exhibit unique biomechanical properties, making traditional uniaxial testing insufficient. Thus, biaxial testing is important because this allows a deeper knowledge of structure-function relationships. Additionally, it provides insight into the axial coupling relationships and often better simulates in-vivo loading states. Also, biaxial testing is important for constitutive modeling in that it allows for a direct measurement of tissue anisotropy. However, biaxial testing is limited by several factors. These include sample geometries, difficulty achieving an equal force distribution in plane, specimen variability, and possible damage due to clamping or fixing the specimen to the device. [1]

The most limiting factor in our biaxial testing device was friction within the system. Because the soft tissues of interest in our laboratory are highly compliant, the amount of friction in the system could not be assumed to be negligible. In order to meaningfully test these tissues, the biaxial testing device needed to be modified to eliminate this source of error.

METHODS

Eliminating friction required a complete redesign of the system. Therefore, several design criteria were developed:

- Friction must be minimized
- A modified strain tracking system must be incorporated to allow custom post-analysis
- A new water bath must be designed to allow testing active mechanical properties
- Longer hooks must be created to attach to the tissue, but do not alter the applied load

After considering the design criteria, the initial design was developed. This design featured four sleds on four tracks, arranged to create two perpendicular axes of motion. Figure 1 depicts the initial design for a sled and track.

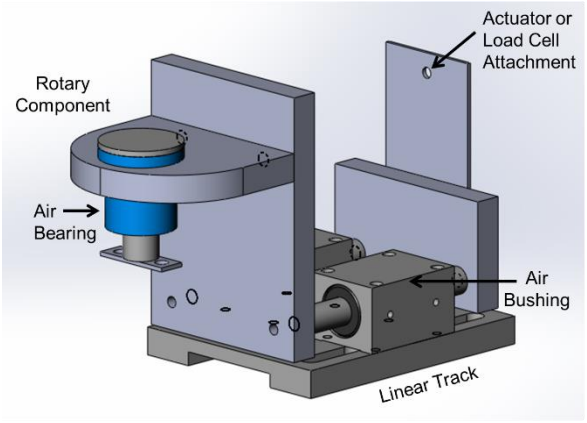

Figure 1: Solidworks drawing for new biaxial testing device design depicting a sled and track

I. Eliminating Friction with Air Bearings

New Way air bearings and bushings were used to combat friction. These air bearings supply pressurized air through a porous media creating a zero contact surface allowing frictionless motion.

II. Air Bearings Validation

To confirm that the air bearings were successfully facilitating frictionless movement, a validation procedure was developed. A load cell was attached to a linear actuator and known masses were displaced on the track in

a sinusoidal waveform. The corresponding function for the displacement waveform was found using Mathematica and the acceleration waveform was

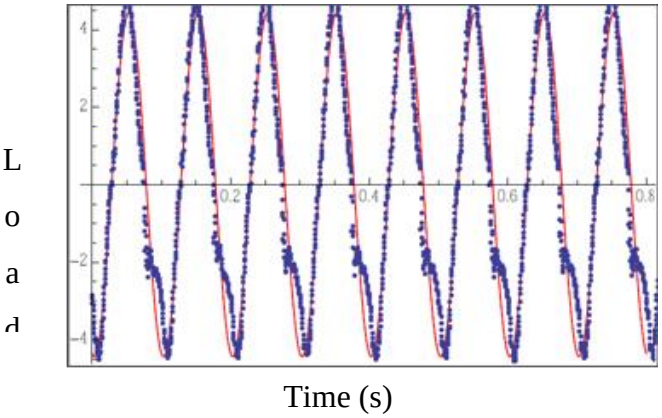

Figure 3: Comparison of the calculated theoretical force (red) and the measured force (blue) from the load cell during validation procedure

subsequently calculated. The maximum theoretical force was then determined using Newton's second law and compared to the maximum force measured by the load cell.

VI. Hook Development

Due to the addition of the linear track, the new hook design required a much greater length than the original hooks. The design for the hooks was fabricated from suture and small fly fishing hooks. This resulted in a long segment of suture with a hook attached by a surgical knot at each end. Small pieces of cork were placed on the hooks making them buoyant. The hooks were attached to the device by wrapping the suture around a spindle connected to the rotary component. This method allows in plane shear and does not restrict the hooks.

VII. Preliminary Hook Testing

To test this hook design, preliminary testing was conducted using the new biaxial testing device and rat skin samples. The samples were approximately 2 cm x 2 cm. Four hooks, two sets of two, were attached to each side of the sample. The protocol applied an equal displacement of four millimeters on each axis.

RESULTS

The new biaxial testing device, including the new water bath, is shown below in Figure 2.

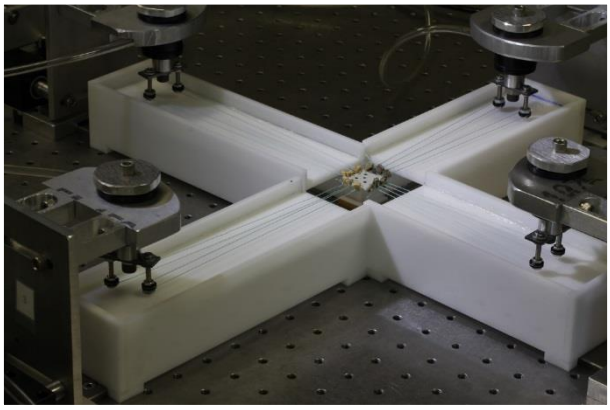

Figure 2: New biaxial testing device with new water bath

I. Air Bearings Validation

The validation procedure has been performed on one sled. The comparison of the theoretical force sinusoid and the measured force sinusoid is displayed in Figure 3.

This procedure revealed a percent difference between measured and theoretical force of approximately 2.46% after neglecting the inertial forces from moving the load cell on the actuator.

II. Preliminary Hook Testing

Preliminary testing of the hooks revealed that suture was not an ideal material. The suture would initially transfer tension to the tissue. However, after returning the specimen to its zero displacement position, the suture would become slacked, indicating a permanent plastic deformation.

DISCUSSION

In this project, we determined that the original biaxial testing device was unsuitable for highly compliant soft tissues. Determining its major weakness as friction, we developed a design for a new biaxial testing device to eliminate friction as well as introduce several other improvements.

The new design satisfies multiple design criteria. The air bearing validation indicates that friction is negligible in the new design. Additionally, both a modified strain tracking system and a new water bath have been incorporated into the system. These improvements over the previous system allow for more accurate testing of highly compliant tissues, and a higher level of control over the data being collected.

The remaining limitation in the system is the deformability of the hooks, resulting in failure to meet all

of the design criteria at this point in time. In the future, it is important to develop a new hook design that is resistant to plastic deformation, able to float, and accommodate small sample sizes. Additionally, further validations should be performed on the air bearings to confirm that the friction in the other sleds is negligible as well.

REFERENCES

1. Sacks, M. 2001. Biaxial Mechanical Evaluation of Planar Biological Materials. *Journal of Elasticity,* 61: 199-246.

ACKNOWLEDGMENTS

Thank you to Katrina Knight and the Musculoskeletal Research Center for their mentoring and support as well as Dean Shuman for providing summer research funding.

Musculoskeletal Research Center
Department of Bioengineering
405 Center for Bioengineering
300 Technology Dr.
P.O. Box 71199
Pittsburgh, PA 15219
http://www.pitt.edu/~msrc